0026-895X/89/050766-07$02.00/0

MOLECULAR PHARMACOLOGY, 36:766-772

Distance Geometry of α-Substituted 2,2-Diphenylpropionate Antimuscarinics

RICHARD K. GORDON, ELI BREUER,[1] FELIPE N. PADILLA, RUTHANN M. SMEJKAL, and PETER K. CHIANG

Department of Applied Biochemistry, Walter Reed Army Institute of Research, Washington, D. C. 20307-5100

Received July 20, 1987; Accepted August 8, 1989

SUMMARY

Quantitative structure-activity relationships between pharmacological activities and physical properties of a series of 2,2-diphenylpropionate compounds were used to define the topography of the antagonist binding site of muscarinic receptors. XICAMM, a computer molecular modeling program, was used to calculate geometrical and topological values of the compounds. The compounds were tested for their antimuscarinic activities by: (a) inhibition of [*N-methyl*-^{3}H]scopolamine binding to the muscarinic receptors of N4TG1 neuroblastoma cells, (b) inhibition of carbachol-induced α-amylase release from rat pancreas acini, and (c) blocking of acetylcholine-induced contraction of guinea pig ileum. To evaluate as clearly as possible only the effect of the bond distance on the potency of the synthesized antimuscarinics, the compounds contained as many constant features as possible. Neither the hydrophobic nor the ester moieties of the compounds were changed, and the rings containing the protonated nitrogen were saturated and restricted. The antimuscarinic activities obtained from the three assays were significantly correlated with each other, with the exception of two compounds, **9** and **13**. The latter two compounds demonstrated specificity for the m3 muscarinic receptor subtype expressed in the pancreas. Furthermore, it was demonstrated that the antimuscarinic activities were significantly related to the bond distances between the carbonyl oxygen (constant electronegative locus) and the protonated nitrogen (center of cationic charge) of the 2,2-diphenylpropionate compounds. Parabolic relationships between the pharmacological activities and bond distances were empirically established. The shortest calculated bond distance of these compounds was approximately 4.4 Å, whereas the longest was about 5.9 Å. The maximum antimuscarinic potency was observed with a calculated bond distance of about 5.2 Å in all three assays.

The interaction of agonists and antagonists with muscarinic acetylcholine receptors (1) may be explored by a variety of means, for example, energy minimization models using molecular mechanics (2), X-ray crystallography (3), and NMR spectroscopy of compounds interacting with solute molecules (4). However, a definitive conformation of the receptor-bound cholinergic ligand has not been established. Several key functional groups are required in a molecule to achieve potent anticholinergic properties (2, 5). A protonated nitrogen atom (the center of the cationic region) should be present at one end of an antagonist molecule, an ester group (the center of the electronegative region) is near the middle of the compound, and a bulky hydrophobic and lipophilic portion is found at the opposite end (6).

Conformationally restricted analogs of benactyzine have been used to characterize the spatial conformation that these molecules assume when binding to the muscarinic receptor (7). Amino esters of α-substituted phenylacetic acid have been synthesized to describe the rather strict size limits of the hydrophobic region of the muscarinic receptor (8). One of the more straightforward means of comparing the structure of antagonists with their potency is to determine the distance between significant pairs of atoms in each antagonist. For example, an "ensemble approach" has been described for the distance geometry analysis for the nicotinic receptor (9). However, correlation of the structure of an antagonist with its potency may be complicated because the antagonist could display different affinities for receptor subtypes. Muscarinic receptors have been classified into five subtypes based on three criteria: (a) selective antagonists, (b) differential effector coupling of cholinergic responses, and (c) gene sequencing (10–12).

In this study, we used distance geometry analysis to describe the preferred linear distance between the carbonyl oxygen (constant electronegative center) and the protonated nitrogen (the locus of the cationic charge) of a series of muscarinic antagonists for optimal interaction with the muscarinic receptor(s). Fifteen antimuscarinic compounds containing the same hydrophobic ester moiety, 2,2-diphenylpropionate, were analyzed (Fig. 1). The effect of changing the bond distance between the protonated nitrogen (located within relatively rigid and saturated rings) and the carbonyl oxygen of the ester was assessed by determining whether the binding of the antagonists to the muscarinic receptor(s) was diminished or increased.

[1] National Research Council Senior Associate, on leave from the Department of Pharmaceutical Chemistry, Hebrew University of Jerusalem, Jerusalem, Israel.

ABBREVIATION: NMS, [*N-methyl*-^{3}H]scopolamine.

Materials and Methods

Pharmacology

Assay of muscarinic receptors in N4TG1 neuroblastoma cells. N4TG1 neuroblastoma cells were cultured and then prepared in Hanks' medium containing 25 mM potassium phosphate (pH 7.4), as described previously (13). Briefly, to assay the inhibition of [^{3}H]NMS binding, triplicate samples of about 1×10^6 cells in 0.25 ml of medium were incubated with each of the compounds to be tested (Fig. 1) and 2 nM [^{3}H]NMS (72 Ci/mmol; NEN-Dupont, Boston, MA.), for 45 min at 25°, in a 96-well plate with agitation. Atropine (10 μM) was added to account for nonspecific binding at all drug doses. To terminate the assay, the cells were collected onto glass fiber filters with a cell harvester and washed with cold phosphate-buffered saline, and the radioactivity was determined afterwards. Pirenzepine was obtained from Research Biochemicals, Inc. (Natick, MA) and AF-DX 116 was a kind gift from Boehringer Ingelheim Pharmaceuticals, Inc. (Ridgefield, CT).

Cholinergic secretagogue assay of dispersed pancreas acini. Pancreas acini were prepared from male Wistar rats as previously described (14). Briefly, three successive treatments of the pancreas with collagenase (0.8 mg/ml; Sigma Chemical Co., St. Louis, MO), followed by suspension in 16 ml of Dulbecco's medium (GIBCO, Grand Island, NY) containing 0.2% albumin, 0.01% trypsin inhibitor, and 0.09% theophylline (Sigma), yielded acini with greater than 99% viability as determined by trypan blue exclusion. To test the antimuscarinic activity of the compounds, varied doses of the compounds were incubated with the cells in the presence of 10 μM carbachol in 0.5 ml. The α-amylase secreted by the acini was measured with the Phadebas kit (Pharmacia Fine Chemicals, Piscataway, NJ).

Guinea pig ileum contraction assay. Sections of ileum from male albino guinea pigs were suspended in Krebs-Ringer buffer at 37° and aerated with 95% O_2 and 5% CO_2. The contractions induced by acetylcholine were recorded with an isometric transducer (Harvard Apparatus, Natick, MA) at 1 g of tension (14).

Data analysis. IC_{50} values, the concentration of the antagonists that inhibited 50% of the [^{3}H]NMS binding to the N4TG1 neuroblastoma cells or produced a 50% decrease of α-amylase secretion in the pancreas acini, were calculated using LIGAND (15), which is a computer program for the analysis of inhibition curves. For the binding assay, K_i values were derived from the IC_{50} values by correcting for receptor occupancy (16) by [^{3}H]NMS; the $K_D = 0.77$ nM. The K_B values were calculated using Schild plot analysis (17). Because pharmacological data are typically distributed normally on a logarithmic scale rather than an arithmetic scale (18), K_i, IC_{50}, and K_B values were converted to log values, pK_i, pIC_{50}, and pA_2, respectively, and the means were tabulated. A computer program performed least squares best-fit curve analysis yielding equation and correlation coefficients (T. S. Cox, Easley, SC). Statistical analysis using the correlation coefficient and t test were supplied by Hewlett Packard (Corvallis, OR).

Molecular modeling. Molecular modeling of the pharmacophores was performed on an IBM XT containing an EGA monitor and a math coprocessor, using a modeling program XICAMM (XIRIS Corp., New Monmouth, NJ). The XICAMM molecular modeling algorithms are based on the classical mechanical approach of Wipke and Dyott (19). There are five potential energy (strain) functions used by the program (20), including (a) a bond-stretching term, (b) a bond angle term, (c) a nonbonded repulsion term or van der Waals' term, and (d) a torsional term. These terms were calculated using a modified Hook's Law. The last term (e) is a hybridization term that forces carbonyl carbons to remain flat and increases the angle between side chains on strained rings. These functions were then minimized using an adaptive steepest descent algorithm designed by XIRIS Corp. to obtain a strain-minimized three-dimensional model of the molecule. Program version 2.0 was used, which, unlike version 1.0, has parameterization for modeling the protonated form of the amines. Thus, the calculations treat the protonated nitrogen as the center of gravity of the positive charge while distributing the charge with its neighborhood atoms, which form the cationic head group.

Chemical Synthesis

General procedures. The 2,2-diphenylpropionates were prepared by reacting 2,2-diphenylpropionyl chloride with the corresponding amino alcohol. Several different methods were utilized to prepare the compounds, depending on the structure of the amino alcohol used. For the biological experiments, the free bases were dissolved in 0.01 M hydrochloric acid, and these solutions were diluted as required. Compounds **4**, **7**, and **9**[2] were obtained on contract from Research Triangle Institute (Research Triangle Park, NC) (F. Ivy Carroll).

Method 1. Synthesis of 10. A solution of 0.01 mM 2,2-diphenylpropionyl chloride in 10 ml of dichloromethane was mixed with a solution of 0.02 mM amino alcohol in 10 ml of dichloromethane and cooled. The mixture remained at 25° for 48 hr.

To purify the product, the reaction mixture was stripped of solvent and the residue was dissolved in 1 N hydrochloric acid and extracted three times with ether. The aqueous acidic solution was basified with a 50% sodium hydroxide solution with cooling. The base liberated by this treatment was extracted by ether. The ether solution was washed three times with distilled water to remove the unreacted amino alcohol. The solvent was dried and evaporated, and the residue was distilled in a short-path distillation apparatus at high vacuum. The yields varied between 50 and 75%. The compounds were characterized by elemental analysis (Spang Micro Analytical Laboratory, Eagle Harbor, MI) and were correct within 0.4%. NMR and IR spectrometry of the synthesized products showed results without any unusual features and were fully consistent with their expected structures.

Method 2. Synthesis of 2, 3, and 8. To 0.05 mol of 2,2-diphenylpropionyl chloride was added 0.075 mol of amino alcohol in 20 ml of pyridine containing 0.5 g of 4-pyrrolidinopyridine. The solution remained at 25° for 3 days. Subsequently, the pyridine was removed by evaporation under high vacuum. Further sample cleanup followed the purification procedure described above. Contaminating traces of pyridine, when present, were removed by heating the product on a steam bath at high vacuum for 30 min.

Method 3. Synthesis of 1, 5, 6, 11, and 12. This method followed Method 2 in all respects except that the reaction mixture was heated at 100° in an oil bath for 24 hr.

Method 4. Synthesis of 13. This compound was prepared as previously described (21).

Method 5. Synthesis of 14. To a solution of 12 ml of ethyl isonipecotate in 240 ml of acetonitrile, 32 ml of formaldehyde solution (37% in water) was added, followed by 8 g of sodium cyanoborohydride. After stirring for 1 hr at ambient temperature, the reaction mixture was neutralized with glacial acetic acid and stirred for a further 45 min while the pH was maintained neutral with the occasional addition of acetic acid. The solvent was removed *in vacuo*, and the excess acetic acid was neutralized by the addition of a small amount of water saturated with potassium carbonate. The solution was extracted with dichloromethane, which was also washed with the potassium carbonate, then dried, and evaporated. The residue, ethyl *N*-methylisonipecotate, was purified by distillation.

A solution of 8.2 g of ethyl *N*-methylisonipecotate in dry ether was added dropwise, with cooling, to a suspension of 5 g of lithium aluminum hydride in 300 ml of ether. After refluxing for 2 hr and then standing overnight at ambient temperature, the excess hydride was decomposed by the addition of 10 ml of water. The solution was filtered, the ether filtrate was dried over magnesium sulfate, the solvent was evaporated, and the residue, *N*-methyl-4-piperidylmethanol, was purified by distillation. This product was then esterified to 2,2-diphenylpropionyl chloride, as described in Method 2, to yield the desired ester, **14**.

[2] We are grateful to Dr. Robert H. Engle, Department of Medicinal Chemistry, Walter Reed Army Institute of Research, Washington, DC 20307-5100 for forwarding this compound.

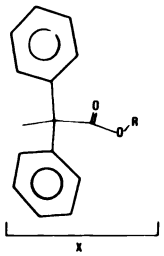

COMPOUND		COMPOUND	
1.	N–ethyl–3–piperidyl–	8.	N–methyl–3–piperidylmethyl–
2.	N–methyl–2–piperidylmethyl–	9.	2–methyl–2–azabicyclo[3.3.1]–nona-7α–yl–
3.	N–methyl–3–pyrrolidinyl–	10.	N–methyl–2–pyrrolidinethyl–
4.	1–pyrrolidineethyl –	11.	N–methyl–4–piperidyl–
5.	1–azabicyclo[2.2.2]–octane–3α–ol–	12.	N–ethyl–4–piperidyl–
6.	8–methyl–8–azabicyclo[3.2.1]–octane–3α–ol–	13.	6–methyl–6–azabicyclo[3.2.1]–octane–3α–ol– (Azaprophen)
7.	1–piperidineethyl –	14.	N–methyl–4–piperidinemethyl –
		15.	N–methy–4–piperidineethyl –

Fig. 1. Structures of the 2,2-diphenylpropionate compounds.

Method 6. Synthesis of 15. To a solution of 11 ml of ethyl isonipecotate in 50 ml of acetone, 24 ml of ethyl iodide were added, and the reaction mixture was allowed to stand at ambient temperature for 24 hr. After evaporation of the solvent and excess ethyl iodide, the residue was suspended in 200 ml of dry ether and 7.5 g of lithium aluminum hydride were added in small portions with cooling during 30 min. The solution was refluxed for 4 hr and allowed to remain at ambient temperature for 24 hr, and then the excess hydride was decomposed by the addition of 10 ml of water. The resulting solution was filtered and the precipitate was washed with ether. The combined ether solutions were dried over magnesium sulfate, filtered, and evaporated, and the residue, *N*-ethyl-4-piperidylmethanol, was then purified by distillation. This product was then esterified to 2,2-diphenylpropionyl chloride, as described in Method 2, to yield the desired ester, **15**.

Results

Computer modeling. After the 2,2-diphenylpropionate portion of each compound (Fig. 1) was modeled by the XICAMM computer program, the amino alcohol portion was added. Then the compound was modeled by the program without restrictions, so that all parts of the combined molecule were free to reach their low energy state. The modeling was performed with the nitrogen of each compound in the protonated (quaternary)

form, where the positive charge is spread out to the neighboring atoms. Bond distances were calculated for each compound between the carbonyl oxygen (the center of gravity of the negative charge) and the protonated nitrogen (the center of gravity of the positive charge) in the preferred configuration modeled by the program (Table 1). Whereas the bond distances of synthesized compounds **1–15** were theoretically calculated by the modeling program on energy-minimized structures, the derived bond distance of **13** has been verified by X-ray crystallography (see Discussion).[3]

Inhibition of [^{3}H]NMS binding to muscarinic receptors of N4TG1 neuroblastoma cells. The antimuscarinic potencies of compounds **1–15** (Fig. 1) were determined by their inhibition of the binding of the muscarinic antagonist [^{3}H]NMS to N4TG1 neuroblastoma cells. The IC_{50} values obtained from the fit of the data were corrected for receptor occupancy (16), yielding pK_i values (Table 1). The compounds inhibited [^{3}H]NMS binding in a concentration-dependent manner (not shown), and these compounds demonstrated competitive inhibition of the muscarinic receptor, with slopes not significantly different from 1.

To determine which subtype of muscarinic receptor is present in the N4TG1 neuroblastoma cells, two selective antagonists were used, pirenzepine and AF-DX 116. Pirenzepine showed low affinity and competitive inhibition, yielding a pK_i of 5.95 M (not shown). AF-DX 116 showed higher affinity; a pK_i of 6.55 M was obtained.

Inhibition of carbachol-induced α-amylase release from pancreas acini. Carbachol binds to muscarinic receptors in dispersed rat pancreas acini and, after a cascade of events, modulates the release of α-amylase (23). This stimulation is a cholinergic response inhibitable by atropine. The compounds inhibited the release of α-amylase in a dose-dependent and competitive manner, because the slopes were not significantly different from 1; the pIC_{50} values are reported in Table 1.

Inhibition of acetylcholine-induced guinea pig ileum contraction. In the third biological assay, the inhibition of acetylcholine-induced contraction of guinea pig ileum by the compounds was measured. Schild plots of the dose-dependent inhibition curves yielded pA_2 values recorded in Table 1. The slopes of the Schild plots approached unity, indicating competitive inhibition (17).

Relationship between the bond distance and pharmacological inhibition data. Table 1 shows a summary of the pK_i, pIC_{50}, and pA_2 values obtained from the muscarinic inhibition assays and the bond distances calculated between the centers of charge, the protonated nitrogen (N^+) and the carbonyl oxygen (C=0), of the compounds by the modeling program. Many, although not all, quantitative correlations between biological activities and structure yield gaussian-like distributions. Parabolic relationships were empirically established between the bond distances and the antimuscarinic potencies of the 2,2-diphenylpropionate compounds in the three antimuscarinic assays: (a) the pK_i values determined from the inhibition of [^{3}H]NMS binding to the muscarinic receptors of the N4TG1 neuroblastoma cells (Fig. 2); (b) the pIC_{50} values determined from the inhibition of α-amylase release (Fig. 3); and (c) the pA_2 values determined from the inhibition of ileum contraction (Fig. 4). The empirical equations defining these three parabolas and their regression coefficients (r) and the significance were, respectively: $y = -76.7 + 32.8X - 3.15X^2$ ($r = 0.90$, $p < 0.001$); $y = -86.8 + 35.9X - 3.42X^2$ ($r = 0.84$, $p < 0.001$); and $y = -51.6 + 22.9X - 2.19X^2$ ($r = 0.78$, $p < 0.001$). Based on the equations defining the three parabolas drawn in Figs. 2, 3, and 4, the calculated bond distance for the maximum antimuscarinic potency was 5.20 Å for the [^{3}H]NMS binding assay, 5.25 Å for the α-amylase release, and 5.24 Å for the ileum contraction. In all three assays, compound **1** was the least potent and had the shortest bond distance, whereas compound **15** had the

TABLE 1

Biological assay and modeled bond distance values

Values are mean ± standard error of three to six replicates.

Compound	[^{3}H]NMS binding, pK_i	α-Amylase release, pIC_{50}	Ileum contraction, pA_2	Bond distance[a]
	M	M	M	Å
1	6.30 ± 0.03	5.63 ± 0.05	6.72 ± 0.04	4.43
2	6.85 ± 0.06	5.57 ± 0.04	7.38 ± 0.01	4.45
3	7.85 ± 0.04	6.05 ± 0.05	7.62 ± 0.01	4.65
4	8.19 ± 0.04	6.81 ± 0.06	7.30 ± 0.03	4.68
5	8.24 ± 0.02	7.36 ± 0.05	8.33 ± 0.02	4.82
6	8.42 ± 0.02	7.08 ± 0.04	8.35 ± 0.02	4.83
7	8.21 ± 0.02	7.11 ± 0.07	7.89 ± 0.09	4.88
8	7.82 ± 0.03	6.53 ± 0.03	7.21 ± 0.01	4.90
9	8.35 ± 0.06	8.36 ± 0.06	8.00 ± 0.04	4.95
10	7.96 ± 0.06	7.52 ± 0.07	8.01 ± 0.03	5.10
11	8.70 ± 0.04	7.02 ± 0.05	8.92 ± 0.03	5.11
12	9.00 ± 0.04	7.86 ± 0.06	8.51 ± 0.02	5.11
13	8.32 ± 0.04	8.31 ± 0.07	8.21 ± 0.06	5.42
14	7.62 ± 0.02	6.93 ± 0.02	7.39 ± 0.02	5.86
15	6.84 ± 0.06	5.82 ± 0.05	7.30 ± 0.02	5.90
Atropine	8.62 ± 0.08	7.36 ± 0.07	8.70 ± 0.08	

[a] Bond distance in angstroms between the protonated nitrogen and the carbonyl oxygen of the modeled compound.

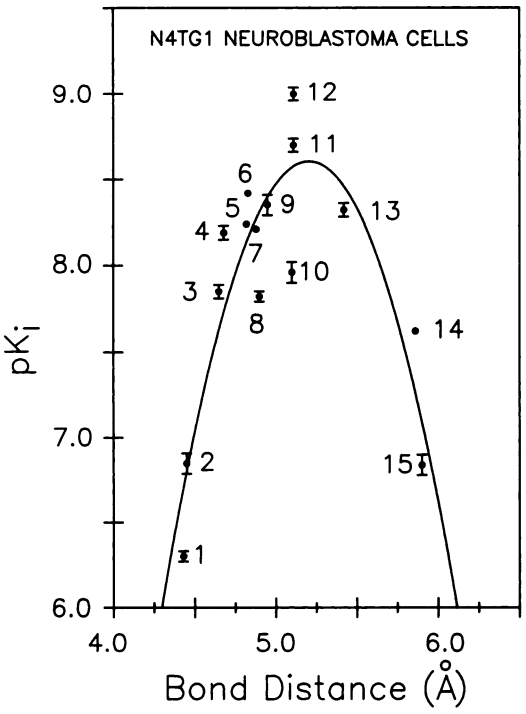

Fig. 2. Parabolic relationship established between the bond distance between the carbonyl oxygen and protonated nitrogen and the pK_i values obtained from the [^{3}H]NMS binding inhibition assay in N4TG1 neuroblastoma cells.

[3] J. M. Karle, I. L. Karle, and P. K. Chiang, unpublished observations.

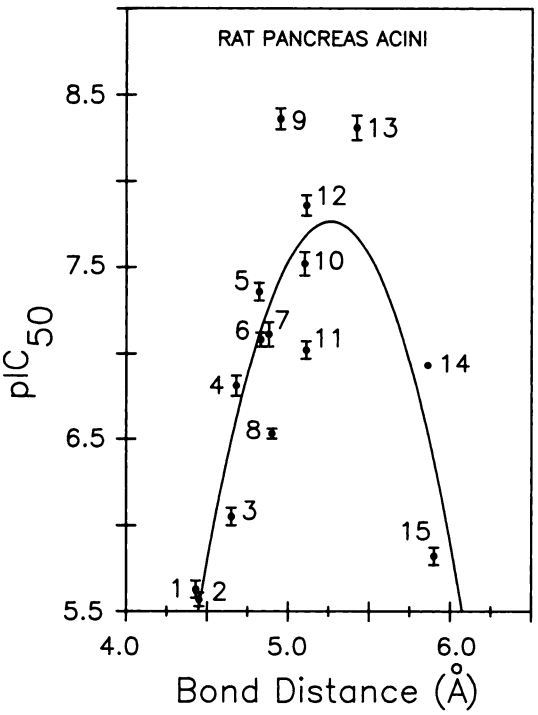

Fig. 3. Parabolic relationship established between the bond distance between the carbonyl oxygen and protonated nitrogen and the pIC_{50} values obtained from the inhibition of α-amylase release in the pancreas acini cells.

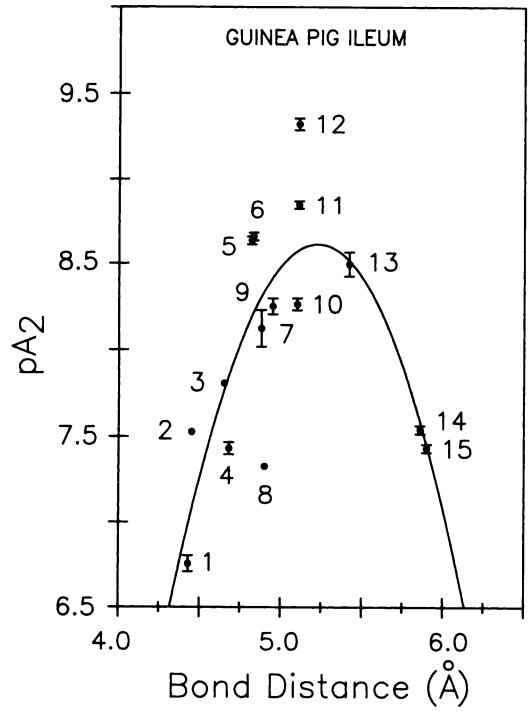

Fig. 4. Parabolic relationship established between the bond distance between the carbonyl oxygen and protonated nitrogen and the pA_2 values obtained from the inhibition of guinea pig ileum contraction assay.

longest bond distance and was one of the least potent antagonists (Table 1; Figs. 2–4).

Relationship between the three pharmacological assays: receptor specificity. The receptor selectivities of the compounds were calculated by using their potencies relative to the nonselective antagonist atropine (Table 2). By determining their relative affinities, a consistent criterion for comparison of receptor selectivity of the compounds may be obtained, because the absolute affinity of each compound could vary depending on the assay (22). With the exception of compounds **9** and **13**, the ratio of the potency of the 13 other compounds in the three pharmacological assays differed by less than 9-fold. Therefore, these compounds showed minimal specificity for the muscarinic receptor subtypes found in the N4TG1 cells, the pancreas acini, or the ileum. On the other hand, whereas compounds **9** and **13** displayed little difference in potency in either the inhibition of [^{3}H]NMS binding or ileum contraction, they were 18- to 50-fold more potent in the inhibition of α-amylase release from pancreas acini. Thus, compound **9** and compound **13** (azaprophen) were more specific for the pancreas muscarinic receptor subtype.

Discussion

Each compound was evaluated using three different pharmacological assays for antimuscarinic activities. First, the [^{3}H]-NMS binding assay in the N4TG1 neuroblastoma cells measured the inhibition of antagonist binding to muscarinic receptors. Nicotinic receptors were undetectable in these cells (24). In the N4TG1 neuroblastoma cells, the m1-selective antagonist pirenzepine showed low affinity (25), a pK_i of 5.95 M, with slope = 1.0. The m2-selective antagonist AF-DX 116 showed higher affinity, pK_i = 6.55 M. However, the slope (Hill coefficient) for the latter was 0.78, indicating that there may be a heterogeneous population of muscarinic receptors in these cells. A related cell line, N18TG1, has the m2 subtype (26). The cerebellum also contains the m2 subtype, and a slope different from unity was observed for AF-DX 116 binding in cerebellum homogenates (27). Taken together, these observations suggest that the muscarinic receptors expressed in N4TG1 neuroblastoma cells were most likely the m2 subtype (12, 22, 27).

TABLE 2

Ratio of potency in biological assays

Ratios of the potencies of the compounds, relative to atropine, in the biological assays from Table 1 are shown. The ratio is defined (22) as:

$$[\text{assay 1/assay 2}] = \text{antilog}\,[(X_{atr} - X_{comp})\ \text{assay 1} - (Y_{atr} - Y_{comp})\ \text{assay 2}]$$

Atr and comp are atropine and the compound to be compared, respectively, and X and Y are pK_i, pIC_{50}, or pA_2 values for assay 1 and assay 2, the two biological assays being compared. Numbers in parentheses are the reciprocal of the ratios. The ratios of the inhibition data in the different tissues were used to indicate receptor selectivity.

Compound	[^{3}H]NMS binding/ α-amylase release	[^{3}H]NMS binding/ ileum contraction	α-Amylase release/ ileum contraction
1	0.3 (3.9)	0.5 (2.2)	1.8
2	1.1	0.4 (2.8)	0.3 (2.9)
3	3.5 (2.3)	2.0	0.6 (1.7)
4	1.3	9.3	7.0
5	0.4 (2.4)	1.0	2.4
6	1.2	1.4	1.2
7	0.6 (1.8)	2.6	3.7
8	1.1	4.9	4.6
9	0.05 (19.)	2.7	50.
10	0.2 (6.7)	1.1	7.1
11	2.6	0.7 (1.5)	0.3 (3.7)
12	0.8 (1.3)	0.7 (1.5)	5.0
13	0.06 (18.)	1.5	27.
14	0.3 (3.7)	2.0	7.6
15	0.6 (1.8)	0.4 (2.4)	0.7 (1.5)

The second assay used pancreas acini cells, which are stimulated by cholinergic agonists to secrete α-amylase. Antagonists inhibit the binding of the agonist carbachol to the m3 muscarinic subtype expressed in the pancreas (12, 28–30). In the third assay, guinea pig ileum contains mainly the m2 subtype of muscarinic receptor (12, 31). However, smooth muscle and most other tissues have been observed to express more than one receptor subtype of mRNA (12). In the three assays, the pK_i, pIC_{50}, and pA_2 values represent the affinities of the antagonists for the muscarinic receptors.

With the exception of compounds **9** and **13**, the compounds showed similar potency profiles in all three assays relative to atropine (22), which is an antagonist that does not discriminate between muscarinic subtypes (Tables 1 and 2). A less than 9-fold difference in potency between the assays might be explained in part by variability in biological assays and different buffer solutions. Binding assays were performed at 25° with N4TG1 neuroblastoma cells, whereas the α-amylase assay was on dispersed pancreas acini at 37° and the ileum contraction assay on ileum sections at 37°. Although some of the differences might also be attributed to low selectivity of the compounds for the receptor subtypes expressed in the different tissues, differences of 5–10-fold may not be considered remarkable between assays (14, 22, 32). There is a very good agreement between the potencies determined from the N4TG1 neuroblastoma binding assay and the ileum contraction assay, which further implies the similarity of the muscarinic m2 receptors expressed in these tissues (Table 2). Mapping of the mRNA from the N4TG1 neuroblastoma cells would further characterize their receptor subtype. A similar relationship among the three assays was observed with another series of antimuscarinic compounds (33). In marked contrast, however, were compounds **9** and **13**, which were approximately 18–50-fold more potent in the pancreas α-amylase assay than in either the N4TG1 cells or ileum assay. Therefore, because compounds **9** and **13** were markedly more potent in inhibiting α-amylase release, both displayed greater selectivity for the m3 muscarinic subtype found in the pancreas acini than the m2 subtype of N4TG1 cells or ileum.

The shortest distance between the protonated nitrogen and carbonyl oxygen in the compounds synthesized was approximately 4.4 Å, whereas the longest was about 5.9 Å (Table 1). The hydrophobic and ester moieties of the compounds were constant, consisting of the fixed 2,2-diphenylpropionate portion. The nitrogen should remain protonated in the assay conditions of pH 7.4. The modified area surrounding the nitrogen was changed in such a way as to introduce as little variability of chemical structures as possible. Also, the rings containing the nitrogen were saturated. In the present series of empirically generated parabolic correlations (Figs. 2, 3, and 4), maximum antimuscarinic potency was achieved with a bond distance of about 5.2 Å in all three assays. Based on X-ray crystallography,[3] **13** was found to have a bond distance between the protonated nitrogen and carbonyl oxygen of 5.41 Å, which is in excellent agreement with its modeled distance of 5.42 Å.

The primary sequence of the m2 muscarinic receptor has been determined recently (11). A hypothetical model for the ligand-binding site of the muscarinic receptor interacting with **11** is shown in Fig. 5. A carboxyl residue (34), possibly an aspartic acid, has been postulated to be involved in the ionic bonding between the anionic binding site of the receptor and

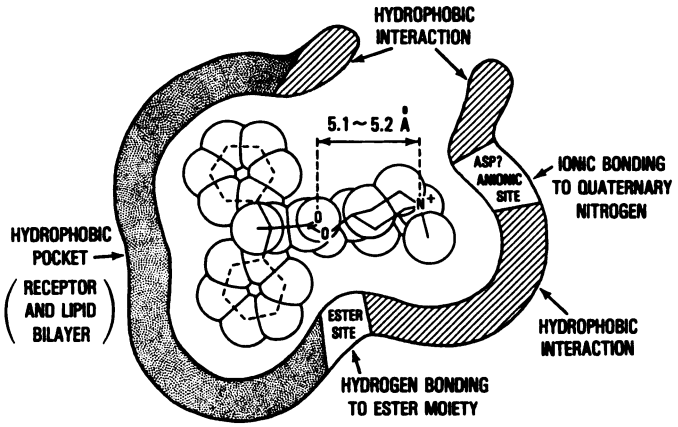

Fig. 5. Representation of a hypothetical model of the ligand binding site of the muscarinic receptor and antagonist **11**. The model illustrates the approximately 5.2 Å bond distance between the protonated nitrogen, shown interacting with the muscarinic receptor's anionic site that may contain an aspartic acid (*ASP*) residue (34), and the carbonyl oxygen, where the ester site of the antagonist could participate in hydrogen bonding with the receptor.

the cationic head group (where the protonated nitrogen is the center of the positive charge) of the antimuscarinic compounds. Notwithstanding the pharmacological differences of the muscarinic receptor subtypes (1), about 65% of the amino acid residues believed to belong to the binding and effector-coupling sites are identical (12, 30). Furthermore, amino acid sequence analysis of the muscarinic receptors also reveals that one of the transmembrane regions in the lipid bilayer of the cell forms a cavity for the hydrophobic residues of the 2,2-diphenyl portion of the tested compounds. In addition, the ester moiety of the antimuscarinic compounds could form a hydrogen bond with the receptor (35).

From a series of relatively planar muscarinic agonists analyzed by Takemura (36), an oxygen site and protonated nitrogen site distance of approximately 5 Å was reported. This distance is similar to the values for antagonists calculated in this report. However, the results reported here are at variance with the statement that the distance between the protonated nitrogen and oxygen atoms could not be an important geometric feature of an antagonist as it is for an agonist (37).

The present investigation provides information on the size constraints of the ligand binding site established by the distance between the ester moiety and the quaternary nitrogen of the 15 antagonists and the corresponding binding sites of the muscarinic receptor. Two of the compounds, **9** and **13**, demonstrated specificity for the m3 muscarinic receptor subtype found in pancreas acini cells rather than the m2 subtype found in N4TG1 cells or guinea pig ileum. The results also demonstrate that potent antimuscarinics can be synthesized and predicted on the basis of distance geometry.

References

1. Nathanson, N. M. Molecular properties of the muscarinic acetylcholine receptor. *Annu. Rev. Neurosci.* **10**:195–236 (1987).
2. Schulman, J. M., M. L. Sabio, and R. L. Disch. Recognition of cholinergic agonists by the muscarinic receptor. 1. Acetylcholine and other agonists with the NCCOCC backbone. *J. Med. Chem.* **26**:817–823 (1983).
3. Chothia, C. Interaction of acetylcholine with different cholinergic nerve receptors. *Nature (Lond.)* **225**:36–38 (1970).
4. Hanisch, P., and A. J. Jones. Carbon-13 magnetic resonance: evidence for non-chair conformations in tropane derivatives. *J. Chem. Soc. Perkin Trans. II*, 1202–1208 (1977).
5. Pratesi, P., L. Villa, V. Ferri, C. De Micheli, M. De Amici, E. Grana, M. G.

S. Barbone, C. Silipo, A. Vittoria, and B. Capello. QSAR in a series of muscarinic agents. *Farmaco. Ed. Sci.* **39**:171–188 (1984).
6. Pauling, P., and N. Datta. Anticholinergic substances: a single consistent conformation. *Proc. Natl. Acad. Sci. USA* **77**:708–712 (1980).
7. Flavin, M. T., C. M. Lu, E. B. Thompson, and H. N. Bhargava. Molecular modification of anticholinergics as probes for muscarinic receptors. 3. Conformationally restricted analogues of benactyzine. *J. Med. Chem.* **30**:278–285 (1987).
8. Lu, C. M., W. E. Wung, L. B. Shih, S. Callejas, J. E. Gearien, and E. B. Thompson. Molecular modification of amino esters of α-substituted phenylacetic acid and related analogs. *J. Med. Chem.* **30**:273–278 (1987).
9. Sheridan, R. P., R. Nilakantan, J. S. Dixon, and R. Venkataraghavan. The ensemble approach to distance geometry: application to the nicotinic pharmacophore. *J. Med. Chem.* **29**:899–906 (1986).
10. Mutschler, E., U. Moser, J. Wess, and G. Lambrecht. New approaches to the subclassification of muscarinic receptors, in *Recent Advances in Receptor Chemistry* (C. Melchiorre and M. Giannella, eds.). Elsevier Science Publishers, Amsterdam, 195–217 (1988).
11. Peralta, E. G., J. W. Winslow, G. L. Peterson, D. H. Smith, J. Ashkenazi, J. Ramachandran, M. I. Schimerlik, and D. J. Capon. Primary structure and biochemical properties of an M_2 muscarinic receptor. *Science (Wash. D. C.)* **236**:600–605 (1987).
12. Buckley, N. J., T. I. Bonner, C. M. Buckley, and M. R. Brann. Antagonist binding properties of five cloned muscarinic receptors expressed in CHO-K1 cells. *Mol. Pharmacol.* **35**:469–476 (1989).
13. Ahmad, A., R. K. Gordon, and P. K. Chiang. A microtechnique for quantification of detergent-solubilized muscarinic and nicotinic acetylcholine receptors using a semi-automated cell harvestor. *FEBS Lett.* **214**:285–290 (1987).
14. Gordon, R. K., and P. K. Chiang. Antimuscarinic activities of hycanthone analogs: possible relationship with animal toxicity. *J. Pharmacol. Exp. Ther.* **236**:85–89 (1986).
15. Munson, P. J., and D. Rodbard. Computer modeling of several ligands binding to multiple receptors. *Endocrinology* **105**:1377–1381 (1979).
16. Cheng, Y.-C., and W. H. Prusoff. Relationship between the inhibition constant (K_i) and the concentration of inhibitor which causes 50 percent inhibition (I_{50}) of an enzymatic reaction. *Biochem. Pharmacol.* **22**:3099–3108 (1973).
17. Tallarida, R. J., A. Cowan, and M. W. Adler. pA_2 and receptor differentiation, a statistical analysis of competitive antagonism. *Life Sci.* **25**:637–654 (1979).
18. Fleming, W. W., D. P. Westfall, I. S. DeLa Lande, and L. B. Jellett. Log-normal distribution of equieffective doses of norepinephrine and acetylcholine in several tissues. *J. Pharmacol. Exp. Ther.* **181**:339–345 (1972).
19. Wipke, W. T., and T. M. Dyott. Simulation and evaluation of chemical synthesis: computer representation and manipulation of stereochemistry. *J. Am. Chem. Soc.* **96**:4825–4834 (1974).
20. Brugger, W. *Computer Aided Molecular Modeling System, V2.0.* XIRIS Corp., New Monmouth, NJ, E1–E5 (1986).
21. Carroll, F. I., P. Abraham, K. Parham, R. C. Griffith, A. Ahmad, M. M. Richard, F. N. Padilla, J. M. Witkin, and P. K. Chiang. 6-Methyl-6-azabicyclo[3.2.1]octan-3α-ol 2,2-diphenylpropionate (Azaprophen), a highly potent antimuscarinic agent. *J. Med. Chem.* **30**:805–809 (1987).
22. Doods, H. N., M.-J. Mathy, D. Davidesko, K. J. Van Charldorp, A. De Jonge, and P. A. Van Zwieten. Selectivity of muscarinic antagonists in radioligand and *in vivo* experiments for the putative m1, m2 and m3 receptors. *J. Pharmacol. Exp. Ther.* **242**:257–262 (1987).
23. Hootman, S. R., T. M. Picado-Leonard, and D. B. Burnham. Muscarinic acetylcholine receptor structure in acinar cells of mammalian exocrine glands. *J. Biol. Chem.* **260**:4186–4194 (1985).
24. Gordon, R. K., F. N. Padilla, E. Moore, B. P. Doctor, and P. K. Chiang. Antimuscarinic activity of aprophen. *Biochem. Pharmacol.* **32**:2979–2981 (1983).
25. Chiang, P. K., R. K. Gordon, H. W.-K. Yeung, T. Alonso, J. M. Witkin, P. Abraham, and F. I. Carroll. Azaprophen (6-methyl-6-azabicyclo[3.2.1]octane-3α-ol 2,2-diphenylpropionate) as a novel and highly potent antimuscarinic agent. *Soc. Neurosci. Abstr.* **12**:294.13 (1986).
26. Bidaut-Russell, M., and A. C. Howlett. Muscarinic pharmacology of the inhibition of adenylate cyclase in N18TG1 neuroblastoma cells. *Neurochem. Int.* **11**:287–292 (1987).
27. Hammer, R., E. Giraldo, G. B. Schiavi, E. Monferini, and H. Ladinsky. Binding profile of a novel cardioselective muscarine receptor antagonist, AF-DX 116, to membranes of peripheral tissues and brain in the rat. *Life Sci.* **38**:1653–1662 (1986).
28. Melchiorre, C., A. Cassinelli, and W. Quaglia. Differential blockage of muscarinic receptor subtypes by polymethylene tetramines: novel class of selective antagonists of cardiac M-2 muscarinic receptors. *J. Med. Chem.* **30**:201–204 (1987).
29. Korc, M., M. S. Ackerman, and W. R. Roeske. A cholinergic antagonist identifies a subclass of muscarinic receptors in isolated rat pancreatic acini. *J. Pharmacol. Exp. Ther.* **240**:118–122 (1987).
30. Peralta, E. G., A. Ashkenazi, J. W. Winslow, D. H. Smith, J. Ramachandran, and D. J. Capon. Distinct primary structures, ligand-binding properties and tissue-specific expression of four human muscarinic acetylcholine receptors. *EMBO J.* **6**:3923–3929 (1987).
31. Barlow, R. B., and P. Weston-Smith. The relative potencies of some agonists at M_2 muscarinic receptors in guinea-pig ileum, atria, and bronchi. *Br. J. Pharmacol.* **85**:437–440 (1985).
32. Birdsall, N. J. M., and E. C. Hulme. Muscarinic receptor subclasses. *Trends Pharmacol. Sci.* **4**:459–463 (1983).
33. Witkin, J. M., R. K. Gordon, and P. K. Chiang. Comparison of *in vitro* actions with behavioral effects of antimuscarinic agents. *J. Pharmacol. Exp. Ther.* **242**:796–803 (1987).
34. Galron, R., and M. Sokolovsky. Carboxyl residue(s) at the ligand-binding site of rat muscarinic receptors. *Biochem. Biophys. Res. Commun.* **156**:1203–1208 (1988).
35. Bebbington, A., and R. W. Brimblecombe. Muscarinic receptors in the peripheral and central nervous systems. *Adv. Drug Res.* **2**:143–172 (1965).
36. Takemura, S. Geometry of muscarinic agonists. *J. Pharmacobio-Dyn.* **7**:436–444 (1984).
37. Broutsyna, N. B., N. V. Khromov-Broisov, N. A. Losev, B. S. Zhorov, and V. A. Govyrin. Primenenie teoreticheskogo konformatsionnago analiza k reshcheniiu proplemy zavisimosti mezhdu strukturoi i deistviem (Application of theoretical conformational analysis to solving the problem of the relationship between the structure and action of cholinergic blocking agents difacil and benactyzine). *Farmakol. Toksikol. (Mosc.)* **43**:219–230 (1981).

Send reprint requests to: Richard K. Gordon, Department of Applied Biochemistry, Walter Reed Army Institute of Research, Washington, DC 20307-5100.